JOURNAL OF AIRCRAFT
Vol. 29, No. 5, Sept.–Oct. 1992

Two-Fence Concept for Efficient Trapping of Vortices on Airfoils

Vernon J. Rossow*
NASA Ames Research Center, Moffett Field, California 94035

Previous work on the use of a vortex trapped above a wing in order to produce high lift at low angles of attack is extended here. It is first postulated that the optimum way to trap a vortex is to design the airfoil section and wing so that the flow along the vortex core is minimized. It is then shown that a vertical fence both in front of and behind the separation bubble generated by the trapped vortex is an effective way to reduce the mass flow removal and its associated drag to a negligible amount. In order to show that vertical surfaces upstream and downstream of the vortex separation bubble have an opposite effect on the source requirements for vortex trapping, conformal mapping methods are used to obtain the solutions for a variety of simple two-dimensional, inviscid, incompressible flow configurations. Trapped-vortex flowfield solutions for the flow over flat plate and Clark-Y airfoils are then used to demonstrate that the heights of the fences can be tailored to make the required mass withdrawal (and therefore, the drag due to trapping) to be vanishingly small.

Nomenclature

b = span
C_d = drag coefficient, D/qcb
C_l = lift coefficient, L/qcb
c = wing chord or characteristic length
D = drag due to flow into sink
h = step or fence height
L = lift
$\dot{m}$ = strength of external source
q = dynamic pressure, $\rho U_\infty^2/2$
r = radius
r_{oc} = radius of circle in original or circle plane
U_∞ = freestream velocity
u, v = dimensionless velocity components
x, y = distance in streamwise and vertical directions
z = complex variables, $x + iy$
$\bar{z}$ = $x - iy$
α = angle of attack
β_{rk} = fence curvature parameter
Γ = circulation in external vortex
θ = meridian angle
Φ = complex potential, $\phi + i\psi$
ϕ = velocity potential
ψ = stream function

Subscripts
i = image vortex
o = original plane
p = physical plane
x = trapped vortex

Introduction

EFFORTS are continuously being made to find simple ways to convert wings of aircraft from an efficient cruise configuration to one that develops the high lift needed during landing and takeoff. One of the first approaches tried was the use of rotating cylinders embedded in the airfoil surface to enhance the lift directly, or to control the boundary layer for high lift situations.[1–7] Steps were then taken to replace the mechanical complexities of a rotating cylinder with a trapped vortex.[8–20] Another category of trapped-vortex concepts consists of leading-edge devices[21–24] that are also used to enhance the lift by working on the flow near the leading edge of the wing.

The trapped-vortex configuration of interest here (Fig. 1) consist of those wherein the separated region occupied by the vortex covers a large part of the upper surface of the airfoil.[17] The problem with such a high-lift device is that the design of the airfoil and wing surfaces that are needed to promote the formation and stability of the trapped-vortex flowfield are not clearly evident. If these trapped-vortex flowfields can be established, theoretical studies show that section lift coefficients of over 10 can then be achieved.[16–20] The particular theoretical study[17] being extended here analyzed the inviscid, incompressible flow over an airfoil with a fence near the leading edge to promote the development and stability of a vortex/sink flowfield over the upper surface of the airfoil, Fig. 1. A sink was placed at the location of the vortex because it was reasoned that fluid would need to be removed from the vortex core to first form and possibly also to help fulfill the equilibrium condition (i.e., zero velocity) at the location of the trapped vortex. In the actual flowfield, withdrawal of fluid is accomplished by spanwise flow along the vortex core that is pulled by a pressure gradient, or by a pump (or sink) at or near the location of the vortex center.

A fence is placed near the leading edge of the airfoil because it is needed for the formation of the trapped vortex. As the

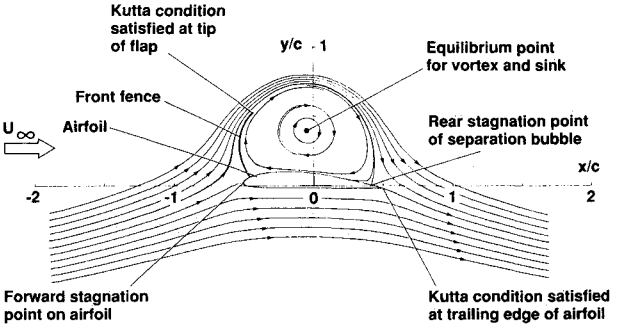

Fig. 1 Flowfield past an airfoil with vortex trapped by a fence near its leading edge.[17]

Received March 3, 1991; revision received Aug. 9, 1991; accepted for publication Aug. 9, 1991.

*Senior Scientist. Associate Fellow AIAA.

fence is first deployed or the airfoil set in motion, the flow separates from the tip of the fence to produce a shear layer that begins to move downstream from the upper end of the fence. The vorticity in the shear layer is concentrated at the location of the sink as fluid is withdrawn. As a result, the vortex strength grows with time until it is strong enough to not only dominate the flow in the separation bubble but also to eliminate the shear layer shed by the front fence. At this stage, the vortex is fully formed so that the flowfield resembles the one presented in Fig. 1. Further withdrawal of fluid at the center of the vortex is then only needed to help render the equilibrium or zero-velocity condition at the center of the vortex. In an actual application, some withdrawal of fluid will probably also be needed to remove low-energy fluid produced by viscous losses.

After the previous theoretical study[17] was completed, experiments were conducted to find out if these trapped-vortex flowfields could actually be established. As predicted by the theory, large amounts of fluid had to be withdrawn from the center of the vortex/sink combination in order to not only establish the flowfield but also to maintain it. For example, a dimensionless sink strength of 0.05 (a weak sink solution[17]; strong sink solutions require 0.5) means that the amount of fluid to be removed per unit time by the sink is equal to a cross-section of the freestream formed by the span and by a height equal to 5% of the chord. Not only is this a large amount of fluid to be drawn from one end of the vortex, but the associated drag is also large because the streamwise momentum of the fluid is removed. Power is also consumed in the evacuation of the vortex unless it is accomplished by the pressure field of the wing. Not as easy to quantify is the disruption of the vortex by the large volume of fluid that must be convected along the core of the vortex to an end where it can be dumped. In the experiments conducted, it seemed fairly obvious that the volume of fluid moving down the core was often so large that it dominated the flowfield to such an extent that a coherent, tightly swirling vortex could not be formed. It was concluded therefore, that if trapped-vortex configurations are to be useable as high-lift devices, some characteristics of the wing or airfoil must be changed so that the vortex is trapped in a way that requires a negligible amount of fluid to be removed from the vortex/sink location for the equilibrium condition. Efficient vortex trapping is then produced when the sink strength is reduced to a negligible amount. The drag due to trapping and the possible need for power to do the pumping are then also negligible. The drag referred to here is only that attributed to the withdrawal of fluid and its momentum exchange. Drag due to viscous forces and due to induced drag are not included.

It is hypothesized therefore, that if an efficient trapped vortex high-lift device is to be achieved, the airfoil (and consequently the wing) should be designed with auxiliary surfaces so that the amount of fluid that must be removed from the vortex core to bring the vortex motion into equilibrium with all of the other induced velocities shall be as near zero as possible. Not only is such a criterion needed for minimization of the drag due to trapping, but it also appears that withdrawal of a large amount of fluid from the vortex core is disruptive of the formation and stability of the vortex. This article concentrates on the use of a vertical surface or fence both in front of and behind the vortex separation bubble, because two such fences are found to be effective and versatile tools for bringing the required mass flow removal rate to zero.

As in the previous study,[17] conformal mapping,[25,26] is used here to generate the inviscid, incompressible, steady-state, two-dimensional flowfields that contain a trapped vortex. A discussion is first presented on the role played by the sink on the vortex-trapping process in order to illustrate why placement of a fence on both the upstream and the downstream end of the separation bubble is an effective means for reducing the amount of sink flow required for equilibrium. Solutions for simple flowfields that contain a trapped vortex are then presented to illustrate how fences, and fore and aft symmetry of the vertical surfaces that border the vortex, affect the magnitude of the source or sink. On the basis of these solutions, it is found that the height, shape, and location of the two fences are not only able to control the size of the trapped-vortex separation bubble but also to form a set of boundaries that make it possible to trap the vortex with negligible mass flow into the vortex center. The results presented here are intended as beginning points for finding versatile fence arrangements which require a minimum mechanical change to wings from their cruise configuration to achieve an efficient trapped-vortex, high-lift wing design for landing and takeoff.

Argument for Fore and Aft Symmetry

The ability of a given configuration to trap a vortex depends on the arrangement of the horizontal and vertical surfaces on which the vortex and source interact, i.e., through the induced velocities of the images of the singularities used to make the solid surfaces into streamlines. Consider first the velocity induced on a vortex by its image beneath a horizontal plane (Fig. 2). Such an interaction permits the vortex to remain stationary against an oncoming stream and thereby establish a steady-state trapped-vortex flowfield. When a vertical surface (i.e., front fence) is placed between the oncoming stream and the vortex, the velocity induced by the primary image of the vortex, which is just upstream of the front fence, is in the upward direction. Unless the flow over and down the back side of the fence exactly compensates this induced vertical velocity component, a source (or sink) must also be placed at the vortex center to induce (through its image) a vertical velocity that compensates for the front image vortex. If, however, a second vertical surface is placed just downstream of the vortex to be trapped, the velocity induced on the vortex by its rear primary image is in the downward direction (Fig. 2). Obviously, if the two vertical surfaces are of about the same size and if the vortex is midway between the two of them, the vertical velocities cancel. Since a sink or source is then not needed to achieve an equilibrium condition, efficient trapping of the vortex has been accomplished. Naturally, inclusion of all of the image vortices (and sinks) in such a simple flowfield and in the more complicated flowfields over airfoils makes the interaction of the vortex with the various surfaces much more complex. However, the general idea of designing fore and aft trapping symmetry into the vertical surfaces by raising or lowering the heights of a front and/or a rear fence will be seen to be an effective means for generating solutions that require a negligible sink strength to trap a vortex.

Before leaving this discussion, it should be noted that surfaces over the top of the vortex are undesireable because the low pressures generated by the vortex flowfield on any overhead areas results in negative lift, which defeats the purpose of the trapped vortex as a high-lift implement. Furthermore, an overhead surface produces an induced velocity contribution from the image vortex that reduces the ability of the trapped vortex to withstand an oncoming airstream.

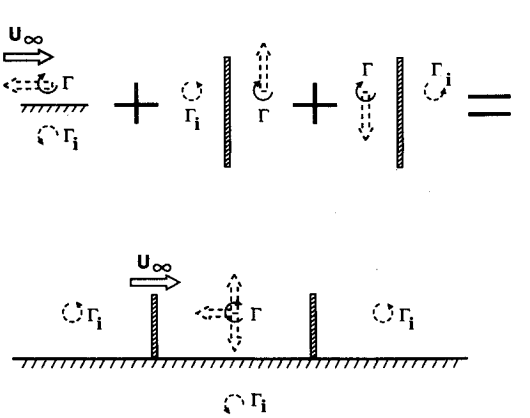

Fig. 2 Image system showing advantage of two-fence concept.

Vortex-Trapping Configurations

In order to gain experience with the vortex trapping process and to enlarge upon the discussion in the previous section, several flowfield geometries are now explored. The primary objective is to gain an intuitive understanding of the effect of vertical surfaces on vortex trapping and on the source flow required for the equilibrium condition. As mentioned in the introduction, conformal mapping techniques[25,26] are used to transform a given flowfield into the desired configuration. The mapping employed takes an initial arrangement of vortices and sources in what is labeled the original plane and then transforms that flowfield by conformal mapping into the physical plane where the desired configuration is studied. The location and strengths of the singularities are determined so that the sum of all the contributions to the velocity at the center of the vortex/source combination sum to zero in the physical plane. In the figures to follow, the streamlines are used to illustrate the flowfield. In order to call attention to the quantity of fluid that enters or leaves the source, which is located at the center of the vortex, those streamlines are crosshatched.

Infinite Flat Plate

The first configuration chosen for study is the infinite flat plate, because it is used as the original flowfield for a number of the cases to follow. A uniform stream is assumed to be moving from left to right past a vortex/source combination situated above the surface a distance, y_{oz}. Since only the infinite horizontal plane is present in the flowfield (Fig. 3a), the velocity induced on the vortex by its image is in a direction parallel to the surface. And, as is well known, the image source induces a velocity in the vertical direction. Therefore, the equilibrium condition for the vortex/source combination specifies that the source vanish and that the strength of the vortex is just large enough that the image-induced velocity is offset by the oncoming freestream velocity:

$$\Gamma = 4\pi y_{ox} U_\infty \tag{1a}$$

$$\dot{m} = 0 \tag{1b}$$

As illustrated in Fig. 3a, a separation bubble is generated on the flat-plate surface at the streamwise location of the vortex. As yet, no feature is present in the flowfield to help generate or to hold the vortex in place. Since the flow is inviscid, the separation bubble could be imagined to have thin

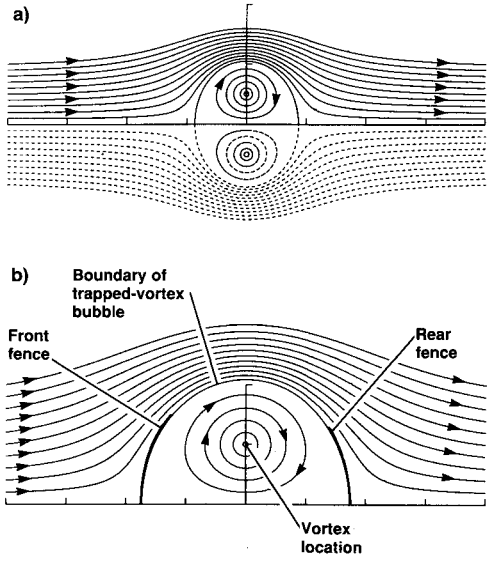

Fig. 3 Trapped vortex on an infinite flat plate; $\Gamma = 4\pi y_{ox} U_\infty$ and $\dot{m} = 0$: a) image and physical streamlines for trapped vortex flowfield, and b) fences fore and aft that conform to shape of vortex separation bubble.

plates over a portion or all of its surface (Fig. 3b). The results produced by this example do not, however, provide any guidance on how large each of the two conforming fences should be made in order to generate and hold the vortex in place.

The solution for the flow over the infinite flat plate when both a vortex and source are present is used as the flowfield in the original plane for a number of the flowfields to be discussed. The general form of the complex potential is found by superposition of singularities as

$$\Phi = z_o + \frac{\dot{m}}{2\pi U_\infty} \ln[(z_o - z_{ox})(z_o - \bar{z}_{ox})] - \frac{i\Gamma}{2\pi U_\infty} \ln \frac{z_o - z_{ox}}{z_o - \bar{z}_{ox}} \tag{2a}$$

and the velocity as

$$\frac{d\Phi}{dz_o} = u_o - iv_o = 1 + \frac{\dot{m}}{2\pi U_\infty}\left(\frac{1}{z_o - z_{ox}} + \frac{1}{z_o - \bar{z}_{ox}}\right) - \frac{i\Gamma}{2\pi U_\infty}\left(\frac{1}{z_o - z_{ox}} - \frac{1}{z_o - \bar{z}_{ox}}\right) \tag{2b}$$

where z_{ox} is the location of the vortex/source combination in the original plane. The image system is chosen so that the infinite flat plate is a streamline. When the only surface is an infinite flat plate, the complex potential for the original plane and the physical plane are the same.

The streamlines in Fig. 3 and in subsequent figures were calculated by first using the local velocity components to predict an extension of the line. The estimated location is then given a cross-stream correction by use of the streamfunction. This process insures that the calculated streamlines are always on or near the streamlines that they represent.

Flow in a Corner

If a semi-infinite plate is placed in the vertical direction on the horizontal plate so that a corner is formed, the corresponding flowfield can be found by conformal mapping or by the superposition of the original vortex/source combination and three of its images. The geometry approximates a trapped vortex/source combination near the intersection or corner of two large flat surfaces. The boundary conditions on the potential flow solution are that no fluid passes through the boundaries, that the location of the vortex/sink is specified, and that the velocity vanish at its location. The complex potential in the original plane is given by Eq. (2a). The solution when the corner occupies the first quadrant in the physical plane is found by use of the mapping function

$$z_p = \sqrt{z_o} \tag{3}$$

The velocity at the location of the vortex/source combination for the conditions at the equilibrium point is found by use of the equation[17]

$$u_{px} - iv_{px} = (u_{ox} - iv_{ox})(dz_o/dz_p)_{z_{ox}} + \frac{\dot{m} - i\Gamma}{4\pi U_\infty}\left(\frac{d^2 z_o/dz_p^2}{dz_o/dz_p}\right)_{z_{ox}} \tag{4a}$$

or

$$u_{px} - iv_{px} = (u_{ox} - iv_{ox})(dz_o/dz_p)_{z_{ox}} - \frac{\dot{m} - i\Gamma}{4\pi U_\infty}\left[\frac{d^2 z_p/dz_o^2}{(dz_p/dz_o)^2}\right]_{z_{ox}} \tag{4b}$$

where, $(u_{ox} - iv_{ox})$ is found at the equilibrium point z_{ox} from Eq. (2b) in the usual limiting process as

$$u_{ox} - iv_{ox} = 1 + \frac{\dot{m} + i\Gamma}{2\pi U_\infty}\left(\frac{1}{z_o - \bar{z}_{ox}}\right) \tag{4c}$$

In this case, no conditions are placed on the beginning or end of the vortex/source separation bubble. The solution is found by simply specifying, z_{ox}, the location of the vortex/source combination and then finding the strengths of the singularities needed to fulfill the condition of zero velocity at z_{ox} as

$$\frac{\Gamma}{U_\infty} = -\frac{8\pi y_{ox}(2x_{ox}^2 + 3y_{ox}^2)}{4x_{ox}^2 + 3y_{ox}^2} \tag{5a}$$

$$\frac{\dot{m}}{U_\infty} = +\frac{8\pi x_{ox} y_{ox}^2}{4x_{ox}^2 + 3y_{ox}^2} \tag{5b}$$

or, in the physical plane

$$\frac{\dot{m}}{U_\infty} = +\frac{8\pi(x_{px}^2 - y_{px}^2)x_{px}^2 y_{px}^2}{(x_{px}^2 - y_{px}^2)^2 + 3x_{px}^2 y_{px}^2} \tag{5c}$$

The results in Eqs. (5) indicate that the strength of the singularities varies as the first power of distance in the original plane and as the second power in the physical plane. However, the strength of the source depends on where it is located relative to the bisector of the corner (Fig. 4). When the equilibrium point is located right on the line of symmetry between the two planes, the source strength is zero (Fig. 4a). When the equilibrium point moves upstream, the required source strength is negative (Figs. 4b and 4d). Conversely, a downstream shift in position causes the required source to become positive (Fig. 4c). Note that the streamlines that enter or leave the source are cross-hatched to help in the visualization of the amount of fluid involved when the location of the trapped vortex is not optimum. This example and the previous one call attention to the role that the images of the source play on the conditions at the equilibrium point. In the first or infinite flat-plate example, the source strength was zero because it produced an unwanted cross-stream velocity. In the second example, a source or sink of finite magnitude was needed only when fore and aft symmetry became unbalanced.

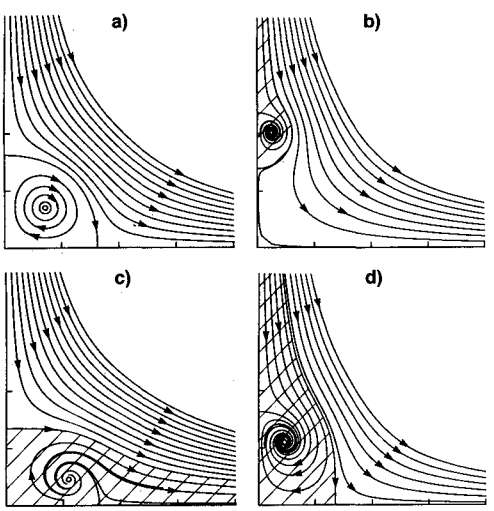

Fig. 4 Streamlines for the flow in a corner located in the first quadrant with a trapped vortex/source combination. Cross-hatched areas denote streamlines entering or leaving source. a) Vortex located on diagonal that bisects corner; $x_{ox} = 0$, $\Gamma/y_{ox}U_\infty = -25.13$, and $\dot{m}/y_{ox}U_\infty = 0$; b) upstream of corner; $x_{ox} = -4$, $\Gamma/y_{ox}U_\infty = -13.13$, and $\dot{m}/y_{ox}U_\infty = -1.50$; c) slightly downstream of corner; $x_{ox} = +1$, $\Gamma/y_{ox}U_\infty = -17.95$, and $\dot{m}/y_{ox}U_\infty = +3.59$; and d) slightly upstream of corner; $x_{ox} = -1$, $\Gamma/y_{ox}U_\infty = -17.95$, and $\dot{m}/y_{ox}U_\infty = -3.59$.

If the trapped-vortex flowfield occurs in the second quadrant rather than in the first quadrant (Fig. 4), the solution simulates the flow on the upstream side of the fence, or the flow approaching a downstream fence. The sign of the vortex remains the same but the sign of the source changes. This result indicates that a downstream fence is able to offset the source strength contribution of the fence located upstream of the vortex separation bubble.

Semi-Infinite Slot

This somewhat fictitious situation is presented to illustrate with a simple geometry the effect of symmetry on the magnitude of the source or sink strength required to bring about the equilibrium condition. It also illustrates just how much variation can occur in the source strength when several boundaries are present. The mapping function used to transform the flow over an infinite flat plate given by Eq. (2) into the flowfield inside the slot is given by

$$z_p = \ell n[z_o + \sqrt{z_o^2 - 1}] \tag{6}$$

where the slot width is two units. Specification of the location of the vortex to be trapped permits substitution of Eq. (6) and its derivatives into Eq. (4b) for the equilibrium conditions. The resulting equations for the strength of the vortex and source were then solved numerically on the computer for each case. Once the unknowns were found, the streamlines were calculated in the original plane and transformed into the physical plane. Some results of the computation are first presented to show the streamlines when a vortex is not present (Fig. 5a) and when a vortex is located midway between the vertical surfaces (Fig. 5b). As expected, when the vortex is located at a point midway between the two vertical surfaces, the required source strength is zero (Fig. 5b). It was found that movement of the equilibrium point upstream a small amount requires a source and a small movement downstream a sink. As the location of the trapped vortex moves to the corners, a point is reached where the source strength passes through zero for equilibrium. Placement of the equilibrium point in either of the corners does not produce a trapped vortex with a source of zero magnitude; note cross-hatched streamlines in Figs. 5c and 5d. As the location of the equilibrium point moves upstream to the corner, the source strength continues to be negative and conversely for movement downstream of the corner. These examples show that a number of locations can be found in the flowfield where the source strength required for equilibrium vanishes, but the best location is midway between the planes. Along such a line the vortex bubble is as large as can be achieved, and the conditions for equilibrium change most slowly with distance.

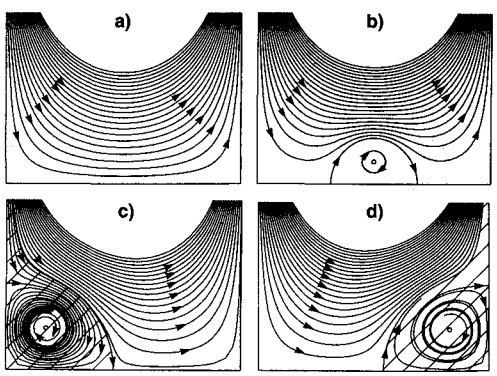

Fig. 5 Examples of flow in a semi-infinite slot in the presence of a trapped vortex; $y_{ox} = +0.3$. Cross-hatched areas denote streamlines entering or leaving source. a) Flowfield without vortex; b) centered between the walls; $x_{ox} = 0$, $\Gamma/bU_\infty = -4.11$, and $\dot{m}/y_{ox}U_\infty = 0$; c) centered in upstream corner; $x_{ox} = -1$, $\Gamma/bU_\infty = -7.77$, and $\dot{m}/y_{ox}U_\infty = -0.38$; and d) centered in downstream corner; $x_{ox} = +1$, $\Gamma/bU_\infty = -7.77$, and $\dot{m}/y_{ox}U_\infty = +0.38$.

Flow over a Step in an Infinite Plane

In the case of a backward facing step, the shear layer that emanates from the upper edge of the step where the flow separates provides the source of vorticity that is concentrated into the vortex by a sink in the lee of the step. This flowfield is also found by conformal mapping of the one shown in Fig. 3. The transformation function used is given by

$$\pi z_p = h(\sqrt{z_o^2 - 1} + \cosh^{-1} z_o) \tag{7}$$

where h is the height of the step which is set equal to one. When Eq. (7) and its derivatives are introduced into Eq. (4b), the strengths of the vortex and sink needed for equilibrium are given by

$$\frac{\Gamma}{U_\infty} = +4\pi y_{ox} \frac{2x_{ox}y_{ox}^2(1 + 2x_{ox}) + (x_{ox}^2 - y_{ox}^2 - 1)^2}{y_{ox}^2(1 - 4x_{ox}^2) - (x_{ox}^2 - y_{ox}^2 - 1)^2} \tag{8a}$$

$$\frac{\dot{m}}{U_\infty} = -4\pi \frac{y_{ox}^2(x_{ox}^2 - y_{ox}^2 - 1)}{y_{ox}^2(1 - 4x_{ox}^2) - (x_{ox}^2 - y_{ox}^2 - 1)^2} \tag{8b}$$

In this case, the boundary conditions to be specified are the location of the vortex/source combination, and that the upstream end of the separation bubble shall be located at the top of the step.

It is found that when the vortex is located near (less than a step height) of the backward facing step, a sink is required to bring about equilibrium of the induced velocities (Fig. 6a). Note that the flow entrained by the sink is cross-hatched. However, when the vortex is located at its optimum location, the required source strength vanishes (Fig. 6b). As the equilibrium point moves further downstream, a source is required (Fig. 6c). When the location moves even further downstream from the step, the strength of the source decreases until it vanishes when the step height is very small compared with the downstream distance. The desired location for the equilibrium point is, naturally, at the downstream distance where the source strength changes sign and is zero because no mass flow is then pulled from the center of the vortex (Fig. 6b, no cross-hatched streamlines). The examples presented for the smaller downstream distances confirm previous predictions that large amounts of fluid must be withdrawn from the vortex for equilibrium when some sort of fore and aft symmetry is not incorporated into the boundaries. The flowfield over a forward facing step (Fig. 6d) is the reverse of that over a backward facing step. Now however, the source becomes positive in order to achieve an equilibrium condition at the location of the trapped vortex, once again illustrating the use of vertical surfaces downstream of the vortex to offset the source strength required by vertical surfaces upstream of the vortex.

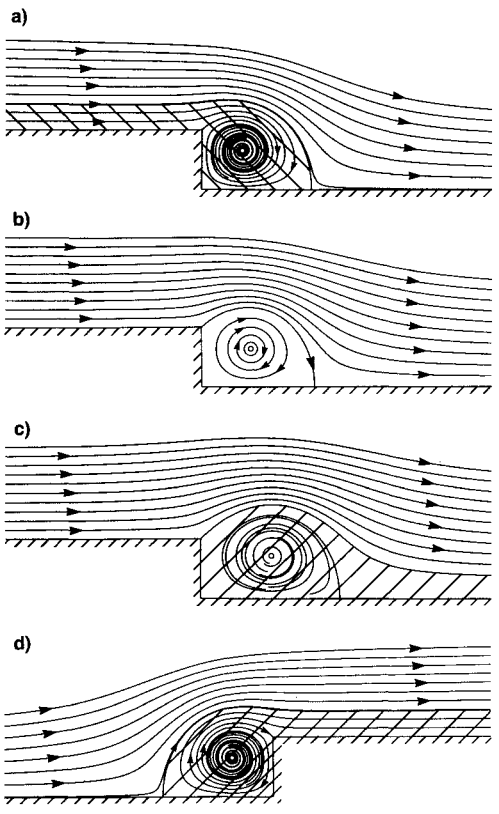

Fig. 6 Flow over step on infinite plane with trapped vortex. Cross-hatched areas denote streamlines entering or leaving source. a) Upstream of ideal location for backward facing step; $x_{px} = +0.68$, $y_{px} = +0.65$, $\Gamma/hU_\infty = -21.31$ and $\dot{m}/hU_\infty = -1.47$; b) at ideal location for backward facing step; $x_{px} = +0.82$, $y_{px} = +0.64$, $\Gamma/hU_\infty = -21.07$ and $\dot{m}/hU_\infty = 0$; c) downstream of ideal location for backward facing step; $x_{px} = +1.18$, $y_{px} = +0.71$, $\Gamma/hU_\infty = -24.00$ and $\dot{m}/hU_\infty = +1.03$; and d) upstream of ideal location for forward facing step; $x_{px} = -0.68$, $y_{px} = +0.65$, $\Gamma/hU_\infty = -21.31$ and $\dot{m}/hU_\infty = +1.47$.

One Fence on Infinite Flat Plate

This example is an idealized approximation of a small fence mounted near the middle of an airfoil. The vortex can be assumed to be trapped either behind or in front of the fence. Once again, the complex potential for the flow over an infinitely long flat plate is used as the solution in the original plane. The solution in the physical plane is obtained by use of the mapping function

$$z_p = \sqrt{z_o^2 - 1} \tag{9}$$

which yields a fence of unit height $h = 1$.

The conditions at the equilibrium point specify that

$$\frac{\Gamma}{4\pi y_{ox} U_\infty} = -1 - \frac{y_{ox}^2(3x_{ox}^2 - y_{ox}^2)}{x_{ox}^2(x_{ox}^2 - 3y_{ox}^2 - 1)^2 + y_{ox}^2(3x_{ox}^2 - y_{ox}^2)(3x_{ox}^2 - y_{ox}^2 - 2)} \tag{10a}$$

When the vortex is trapped downstream of the fence, the tip of the fence serves as a separation point for the oncoming flow so that a vortex/source bubble is formed. This condition specifies that

$$\frac{\dot{m}}{\pi U_\infty} = \left[(x_{ox}^2 + y_{ox}^2) + 2y_{ox}\frac{\Gamma}{2\pi U_\infty}\right] \Big/ x_{ox} \tag{10b}$$

As expected, since a means is not available for any kind of fore-and-aft symmetry, a sink is required at the vortex center for vanishing velocity (Fig. 7). When the equilibrium point is just downstream of the fence (Fig. 7a), a large amount of fluid (see cross-hatched streamlines) must be absorbed by the sink to establish an equilibrium condition. As the location of the vortex moves downstream of the fence, the required sink strength rapidly becomes smaller (Fig. 7b). It was found that when the equilibrium position is only about two fence heights downstream of the fence, the sink strength required for equilibrium is small relative to the size of the separation bubble. In the limit as the vortex location is far downstream relative to the height of the fence, the flowfield becomes like that of the infinite flat plate without a fence.

Since the solution is equally valid if the vortex is assumed to be trapped upstream of the fence, one such solution is presented in Fig. 7c. Even though the fence cannot now serve as a means for producing the vorticity for the vortex, it does show that a fence downstream of the separation bubble brings about a source strength of opposite sign to the one induced

by the upstream fence. These results suggest again that a combination of upstream and downstream fences is an effective way to achieve vortex trapping that requires negligible sink flow. It is also to be noted that the vortex strength is the same whether the vortex is located upstream or downstream of the fence, but the source strength changes sign with position, being negative when the vortex is downstream (Fig. 7b), and positive when the vortex is upstream of the fence (Fig. 7c). This result confirms the previous discussion with regard to the use of a front and rear fence to balance the induced velocities at the vortex and thereby achieve vortex trapping with negligible mass flow removal.

Semi-Infinite Flat Plate

The leading-edge vortices often found on delta wings at high angles of attack suggest that perhaps a special relationship exists between the wing and its ability to trap vortices near its leading edge. An approximation to such a flowfield is made here by considering a section of the wing as a two-dimensional airfoil with a large chord (i.e., a semi-infinite plate) and then look only at the flow near the leading edge. The spanwise flow in the core of the vortex is again simulated by placing a sink (negative source) at the center of the vortex. The present conformal mapping technique permits a solution with the plate at angle of attack.

The flowfield in the original plane once again uses an infinite flat plate as the boundary, but the incident flow is a stagnation point flow rather than a uniform flow along the x axis. The location of the stagnation point on the infinite plane and the incidence angle of the oncoming stream determine the circulation on the semi-infinite plate and the angle of incidence of the oncoming stream in the physical plane. The complex potential for the flowfield in the original plane is then given by

$$\Phi = (z_o - x_{ost})^2 + \frac{\dot{m}}{2\pi U_\infty} \ln[(z_o - z_{ox})(z_o - \bar{z}_{ox})] - \frac{i\Gamma}{2\pi U_\infty} \ln \frac{z_o - z_{ox}}{z_o - \bar{z}_{ox}} \tag{11a}$$

where x_{ost} is the location of the stagnation point of the oncoming stream in the original plane. The general expression for the velocity in the original plane is then given by

$$u_o - iv_o = 2(z_o - x_{ost}) + \frac{\dot{m}}{2\pi U_\infty}\left(\frac{1}{z_o - z_{ox}} + \frac{1}{z_o - \bar{z}_{ox}}\right) - \frac{i\Gamma}{2\pi U_\infty}\left(\frac{1}{z_o - z_{ox}} - \frac{1}{z_o - \bar{z}_{ox}}\right) \tag{11b}$$

The mapping function used to generate the flowfield in the physical plane is given by

$$z_p = z_o^2 \tag{12}$$

The boundary condition requires that the flow is parallel to the plate, that the flow depart smoothly from, or onto, the leading edge of the semi-infinite plate to form the vortex/source bubble, and that the velocity at the equilibrium point vanish. The parameter x_{ost} is used to change the location of the stagnation point on the plate and, consequently, its lift. In order for the velocity to vanish to the location of the vortex/source combination, the following three equations must be satisfied:

$$\frac{\Gamma}{8\pi U_\infty} = -(y_{ox}/x_{ox})(x_{ox}^2 - y_{ox}^2 - x_{ox}x_{ost}) \tag{13a}$$

$$\frac{\dot{m}}{8\pi U_\infty} = +(y_{ox}^2/x_{ox}^2)(2y_{ox}^2 + x_{ox}x_{ost}) \tag{13b}$$

The fact that the flow must separate at the leading edge of the plate yields the condition that

$$x_{ox}\frac{\dot{m}}{2\pi U_\infty} - y_{ox}\frac{\Gamma}{2\pi U_\infty} + x_{ost}(x_{ox}^2 + y_{ox}^2) = 0 \tag{13c}$$

These equations are solved by first choosing a value for the streamwise location of the equilibrium point x_{ox} and for x_{ost}. An iterative process is then used to numerically solve Eqs. (13) for the strengths of the singularities and for the height of the equilibrium point above the plate. The example presented in Fig. 8 illustrates the streamlines for the flowfield. In this particular case, the flowfields for various sizes of vortex bubble are self-similar. Therefore, all of the trapped-vortex configurations require a finite sink.

One Fence on Semi-Infinite Flate Plate

A next step in complexity is formed by using the complex potential in Eq. (11a) with another mapping function

$$z_p = (z_o + 1)\sqrt{z_o^2 - 1}/\lambda \tag{14}$$

The quantity $\lambda = 3\sqrt{3}/4 = 1.299$ is used to cause the mapping to produce a fence at the leading edge of the semi-infinite flat plate of unit height (Fig. 9). Addition of the fence changes

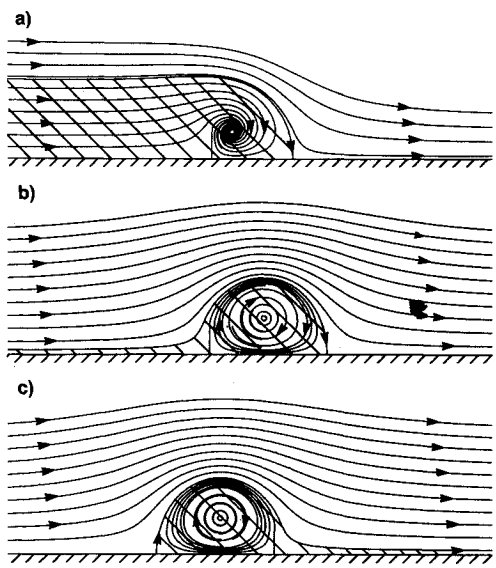

Fig. 7 Flow over a fence on an infinite flat plate with trapped vortex. a) Near top of fence; $x_{px} = +0.67$, $y_{px} = +0.91$, $\Gamma/hU_\infty = -11.67$ and $\dot{m}/hU_\infty = -2.80$; b) downstream of fence; $x_{px} = +1.81$, $y_{px} = +1.21$, $\Gamma/hU_\infty = -15.23$ and $\dot{m}/hU_\infty = -0.15$; and c) upstream of fence; $x_{px} = -1.81$, $y_{px} = +1.21$, $\Gamma/hU_\infty = -15.23$ and $\dot{m}/hU_\infty = +0.15$.

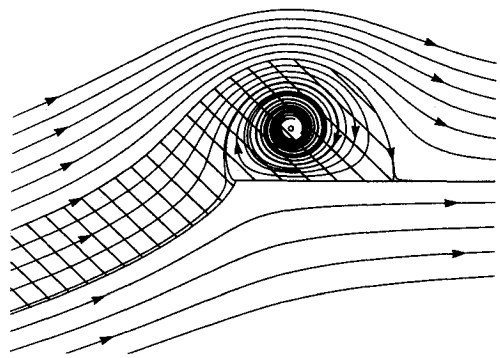

Fig. 8 Flow over semi-infinite plate with trapped vortex; flowfield is self-similar. $x_{ox} = 1.5$, $y_{ox} = 0.58$, $\Gamma/hU_\infty = -31.31$ and $\dot{m}/hU_\infty = -2.46$.

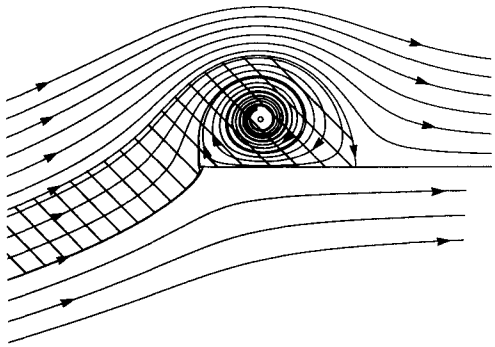

Fig. 9 Flow over semi-infinite flat plate with leading-edge fence that holds a trapped vortex. Cross-hatched areas denote streamlines entering or leaving source. $x_{px} = 2.05$, $y_{px} = 1.59$, $\Gamma/hU_\infty = -36.70$, and $\dot{m}/hU_\infty = -2.66$.

the flowfield a small amount but does not remove the need for withdrawal of a substantial amount of fluid (see cross-hatched streamlines) from the center of the vortex. Although a leading-edge fence will help in the formation of the vortex, it does not appear to be of much help in reducing the strength of the source required for equilibrium.

Two Fences on Flat-Plate Airfoil

The next step in the progression of solutions would be to study either an infinite or a semi-infinite flat plate with two fences. However, the mapping functions needed were too complicated to bring them out of their integral form. Since the flowfield of a flat-plate airfoil with two fences on its upper surface approximates these situations and since it is of direct interest for the understanding of trapped-vortex flowfields on airfoils, it is used as the next example.

The flowfield in the original plane to be used here is the same one studied previously.[17] The complex potential for the flowfield is composed of a superposition of vortex and source singularities to produce a separation bubble on the outside of a circular boundary. A vortex, Γ_o, is also placed at the center of the circle in the original or z_o plane to represent the circulation on the circle. The complex potential is then given by[17]

$$\Phi = (z_o + r_{oc}^2/z_o) + \frac{\dot{m}}{2\pi U_\infty} \ln[(z_o - z_{ox})(z_o - z_{ix})/z_o] - \frac{i\Gamma}{2\pi U_\infty} \ln \frac{z_o(z_o - z_{ox})}{z_o - z_{ix}} - \frac{i\Gamma_o}{2\pi U_\infty} \ln z_o \tag{15a}$$

where r_{oc} is the radius of the circle in the z_o plane and $z_{ix} = z_{ox}r_{oc}^2/r_{ox}^2$ is the location of the image of the vortex/source combination inside the circle. A vortex and a source are also placed at the center of the circle to compensate for the image singularities. The velocity in the flowfield is then found as

$$u_o - iv_o = (1 - r_{oc}^2/z_o^2) + \frac{\dot{m}}{2\pi U_\infty}\left(\frac{1}{z_o - z_{ox}} + \frac{1}{z_o - z_{ix}} - \frac{1}{z_o}\right) - \frac{i\Gamma}{2\pi U_\infty}\left(\frac{1}{z_o - z_{ox}} - \frac{1}{z_o - z_{ix}} + \frac{1}{z_o}\right) - \frac{i\Gamma_o}{2\pi U_\infty}\left(\frac{1}{z_o}\right) \tag{15b}$$

The angle of attack of the airfoil relative to the freestream is imposed on the airfoil by several steps in the mapping sequence.

The magnitude and locations of the singularities are determined so that 1) the front end of the vortex/source bubble maps into the tip of the front fence; 2) the downstream end of the separation bubble maps into the tip of the rear fence; and 3) the trailing edge of the flat plate airfoil is the downstream stagnation point. The locations of these three points on the circle in the z_o plane are found by mapping backwards from the physical plane through the formation of the two fences to the circle in the original plane. In this way, when the zero velocity condition at the equilibrium point is imposed, there are just enough boundary conditions to tie down the magnitude and location of the vortex/source combination at the equilibrium point and the net circulation Γ_o on the circle. The relationship between the singularities in the flowfield and the stagnation points is obtained from the circumferential velocity on the surface of the circle in the z_o plane as

$$v_\theta = -2\sin(\theta_{oc}) + \frac{\dot{m}}{2\pi U_\infty}\left(\frac{2r_{ox}\sin(\theta_{oc} - \theta_{ox})}{r_{oc}^2 + r_{ox}^2 - 2r_{oc}r_{ox}\cos(\theta_{oc} - \theta_{ox})}\right) + \frac{\Gamma}{2\pi U_\infty}\left\{\frac{2[r_{oc} - r_{ox}\cos(\theta_{oc} - \theta_{ox})]}{r_{oc}^2 + r_{ox}^2 - 2r_{oc}r_{ox}\cos(\theta_{oc} - \theta_{ox})}\right\} + \frac{\Gamma_o}{2\pi U_\infty}\left(\frac{1}{r_{oc}}\right) \tag{16}$$

The chord, c, of the flat plate airfoil is taken as one. The details of the mapping are not discussed here because it closely parallels the ones used previously.[17,27]

Only cases wherein the angle of attack of the flat plate airfoil is zero are presented here because the primary purpose of the paper is to illustrate the effectiveness of a second vertical surface or fence on reduction of the source or sink strength required for trapping. Two situations are presented in Figs. 10 and 11 in order to illustrate how the source strength required for the equilibrium condition to be established can be made negligible by adjusting the heights of the front and/or rear fence. Once again the flow entering or leaving the source is cross-hatched. Fig. 10a presents the solution for a vortex/source combination trapped on the upper surface of a flat plate at zero angle of attack without fences. If the vortex bubble had been very small compared with the chord of the plate, the source strength would have been zero. For the configuration shown, the required source strength is quite small but not negligible. Therefore, only a small front fence is required to make the source strength vanishingly small (Fig. 10b).

In order to show how a fairly large front and rear fence offset one another with regard to source strength, a two-fence configuration is presented in Fig. 11. The first solution presented (Fig. 11a) is the one wherein the fence heights have been adjusted to make the source strength zero. In Figs. 11b

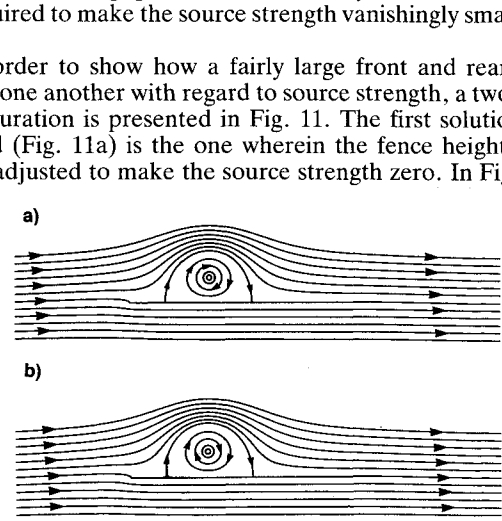

Fig. 10 Vortex trapped on flat plate of finite length; $\alpha = 0$. a) No fences; $h_1/c = h_2/c = 0$; $x_{px} = -0.175$, $y_{px} = +0.102$, $\Gamma/cU_\infty = -1.299$, $\Gamma_o/cU_\infty = +1.095$, $\dot{m}/cU_\infty = +0.004$; $C_l = 0.407$, and $C_d = -0.007$; and b) front fence just large enough to reduce $\dot{m}$ to zero; $h_1/c = 0.0704$, $h_2/c = 0$; $x_{px} = -0.175$, $y_{px} = +0.102$, $\Gamma/cU_\infty = -1.355$, $\Gamma_o/cU_\infty = +1.134$, $\dot{m}/cU_\infty = +0.0$; $C_l = 0.422$, and $C_d = 0.0$.

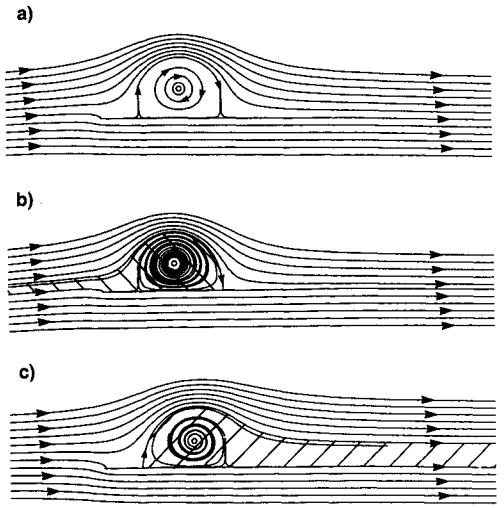

Fig. 11 Effect of presence of fences on source strength required for vortex to be trapped on flat plate of finite length; $\alpha = 0$. Cross-hatched areas denote streamlines entering or leaving source. a) Fence heights determined so that $\dot{m} = 0$; $h_1/c = 0.126$, $h_2/c = 0.121$; $x_{px} = -0.172$, $y_{px} = +0.121$, $\Gamma/cU_\infty = -1.602$, $\Gamma_o/cU_\infty = +1.316$, $\dot{m}/cU_\infty = +0.0$; $C_l = 0.573$, and $C_d = 0.0$; b) front fence only; $h_1/c = 0.126$, $h_2/c = 0$; $x_{px} = -0.202$, $y_{px} = +0.113$, $\Gamma/cU_\infty = -1.479$, $\Gamma_o/cU_\infty = +1.205$, $\dot{m}/cU_\infty = -0.040$; $C_l = 0.548$ and $C_d = 0.0792$; and c) rear fence only; $h_1/c = 0$, $h_2/c = 0.121$; $x_{px} = -0.128$, $y_{px} = +0.110$, $\Gamma/cU_\infty = -1.412$, $\Gamma_o/cU_\infty = +1.248$, $\dot{m}/cU_\infty = +0.099$; $C_l = 0.327$, and $C_d = -0.198$.

and 11c the flow field solutions are presented for the flow over the flat plate with only the front or the rear fence present. It is to be noted that the source strengths (note cross-hatched streamlines) required for each of the fences separately are not equal indicating a nonlinear relationship between the various flowfield parameters and fence height.

Two Fences on Clark-Y Airfoil

The final two-dimensional configuration to be studied consists of the addition of a second fence to the single fence Clark-Y (NACA 4412) airfoil geometry studied previously.[17] That is, if the two-fence concept is to be viable, it should make it possible to bring about vortex trapping with only a vanishingly small sink being required at the vortex equilibrium point. The complex potential and velocity in the circle plane are, of course, the same as Eqs. (15). The mapping sequence used to generate the Clark-Y airfoil with two fences is the same as for the flat plate airfoil except that, instead of a very thin slit, a Clark-Y airfoil[17,28,29] is mapped by the final steps of the mapping sequence. Once again, the location of the stagnation points in the original (or circle) plane are found by mapping the known locations in the physical plane back into the original plane. The procedure is done numerically because the equations are too complicated to carry out the process in closed form.

As with the flat-plate examples, the solution is first found for the Clark-Y airfoil without any fences (Fig. 12a). As mentioned previously, the configuration shown may be considered to have been generated by use of fences that conform to the surface of the vortex separation bubble. Placement of a fence (that is nearly a flat plate) at the rear surface of the trapped vortex is effective in reducing the required source strength to approximately zero. The solution shown (Fig. 12b) was obtained by iterating on the fence height until a height h_2/c is obtained that requires a source strength that is zero to four significant figures.

Figure 13 presents the flowfields over the Clark-Y airfoil with two larger fences, with only the front fence, and with only the rear fence. Once again, each fence separately contributes differently to the source flow requirements needed for equilibrium. However, when both fences are present (Fig. 13a), the sink strength and its associated drag become negligible. When only one fence is present, a sink or a source (see streamlines that are cross-hatched) is required to bring the trapped vortex into equilibrium.

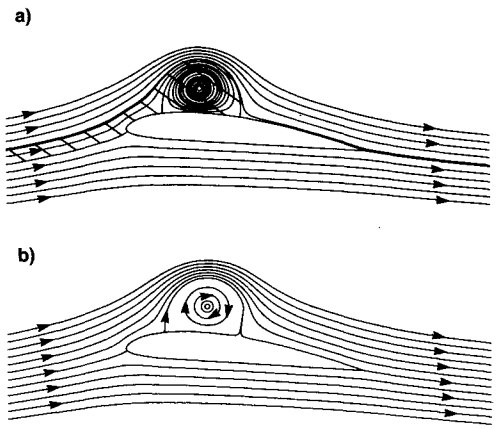

Fig. 12 Vortex trapped on Clark-Y airfoil; $\alpha = 0.1$. a) No fences; $h_1/c = 0$, $h_2/c = 0$; $x_{px} = -0.197$, $y_{px} = +0.216$, $\Gamma/cU_\infty = -1.749$, $\Gamma_o/cU_\infty = +0.869$, $\dot{m}/cU_\infty = -0.054$; $C_l = 1.761$, and $C_d = 0.108$; and b) rear fence just large enough to reduce $\dot{m}$ to zero; $h_1/c = 0$, $h_2/c = 0.114$; $x_{px} = -0.615$, $y_{px} = +0.332$, $\Gamma/cU_\infty = -1.886$, $\Gamma_o/cU_\infty = +0.998$, $\dot{m}/cU_\infty = 0.0$; $C_l = 1.777$, and $C_d = 0.0$.

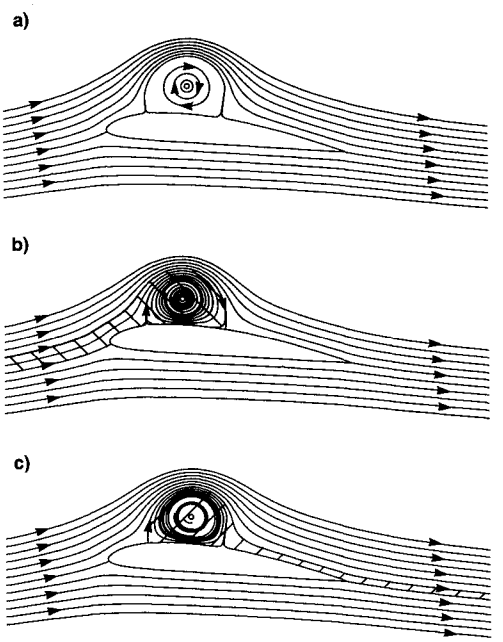

Fig. 13 Effect of presence of fences on source strength required for vortex to be trapped on Clark-Y airfoil; $\alpha = 0.1$. Cross-hatched areas denote streamlines entering or leaving source. a) Fence heights determined so that $\dot{m} = 0$; $h_1/c = 0.064$, $h_2/c = 0.117$; $x_{px} = -0.169$, $y_{px} = +0.226$, $\Gamma/cU_\infty = -1.964$, $\Gamma_o/cU_\infty = +1.053$, $\dot{m}/cU_\infty = 0.0$; $C_l = 1.822$, and $C_d = 0.0$; b) front fence only; $h_1/c = 0.064$, $h_2/c = 0$; $x_{px} = -0.204$, $y_{px} = +0.219$, $\Gamma/cU_\infty = -1.809$, $\Gamma_o/cU_\infty = +0.907$, $\dot{m}/cU_\infty = -0.061$; $C_l = 1.802$, and $C_d = 0.122$; and c) rear fence only; $h_1/c = 0$, $h_2/c = 0.117$; $x_{px} = -0.158$, $y_{px} = +0.222$, $\Gamma/cU_\infty = -1.903$, $\Gamma_o/cU_\infty = +1.026$, $\dot{m}/cU_\infty = +0.024$; $C_l = 1.753$, and $C_d = -0.049$.

Application of Two-Fence Vortex Trapping Concept to Wings

When the two-fence concept is applied to a wing, the results for airfoils should be used as a model for the spanwise design of the fence heights and locations. It should be borne in mind that the vortex must remain intact along the spanwise extent of its use for lift enhancement. Hence, the two fences should extend in approximately straight lines from the origin of the vortex at the fuselage, or centerplane of the wing, to the spanwise station where the vortex is allowed to spill downstream into the wake (Fig. 14a). The inboard end of the fences

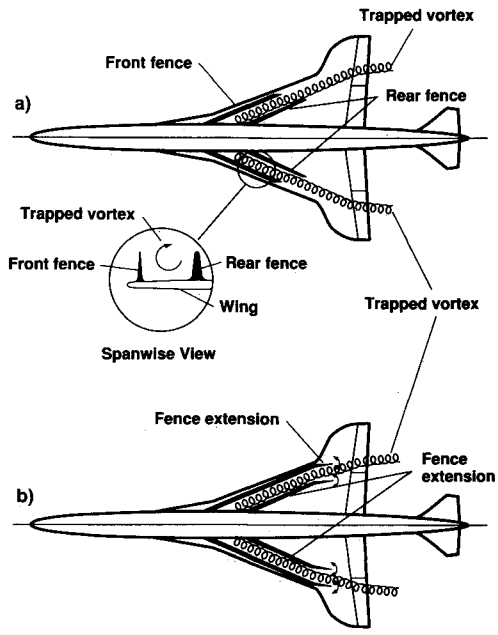

Fig. 14 Plan view of wing showing how the two-fence vortex trapping concept might be applied: a) Fixed spanwise extent of fences; note that top of rear fence is rounded to reduce likelihood of flow separation as flow reattaches behind trapped vortex; and b) configuration with moveable spanwise extensions of fence to vary total lift, rolling moment, and/or pitching moment.

where the vortex begins should abut up against the fuselage to provide a firm ending surface for the vortex. In an actual application, it may be necessary to withdraw fluid at the fuselage end of the vortex as well as at the wingtip end if the design cannot be made to be self driven. Various surfaces may need special treatment to make the trapped vortex function as desired. For example, some rounding to the tip of the rear fence will help to prevent flow separation as the flow reattaches, just in case the rear stagnation point does not line up exactly with the tip of the rear fence. The tip of the front fence should be kept sharp in order to keep the departure of the fluid from it as smooth as possible. Another variation that may be of benefit for changes in lift, pitching moment, and/or rolling moment on the wing is to change the spanwise extent of the trapped vortex by changing the spanwise extent of the fences at their downstream end (Fig. 14b).

Concluding Remarks

The foregoing results demonstrate the effectivensss of the two-fence concept as a means for designing efficient trapped-vortex airfoil configurations. The criterion for an efficient design was that the mass removal from the vortex core for the equilibrium condition should be negligible. Not only is the drag due to the trapping process then negligible, but the trapped vortices should be much easier to form and maintain. The process studied uses adjustments in the height of the front and/or rear fence to bring about efficient trapped-vortex flowfields. The analysis of several simple geometric configurations provide guidance on the trapping process and generate intuition on the conditions that produce trapped-vortex situations. In particular, the configurations studied show that some sort of fore and aft symmetry in the aerodynamics of the vertical surfaces near the vortex is needed to bring about the equilibrium condition without the need for sources and/or sinks.

References

[1]Prandtl, L., and Tietjens, O. G., *Applied Hydro- and Aero-Mechanics,* McGraw-Hill, New York, 1934, pp. 155, 156, 279–287.

[2]Wolff, E. B., "Preliminary Investigation of the Effect of a Rotating Cylinder in a Wing," NACA TM 307, 1925; reprinted from *De Ingenieure*, No. 49, Dec. 6, 1924, pp. 57–66.

[3]Betz, A., "Recent Experiments at Goettingen Aerodynamic Institute," NACA TM 310, 1925; reprinted from *Zeitschrift des Vereines deutscher Ingenieure,* Jan. 3, 1925, pp. 9–14.

[4]Ackeret, J., "Recent Experiments at Goettingen Aerodynamic Institute," NACA TM 323, 1925; reprinted from *Zeitschrift fuer Flugtechnik und Motorluftschiffahrt,* Feb. 14, 1925, pp. 44–52.

[5]Wolff, E. B., and Konig, C., "Tests for Determining the Effect of a Rotating Cylinder Fitted into the Leading Edge of an Airplane Wing," NACA TM 382, 1926; reprinted from Rept. A.105 of the Rijks-Studiedienst Voor de Luchtvaart, Amsterdam.

[6]Frey, K., "Experiments with Rotating Cylinders in Combination with Airfoils," NACA TM 382, 1926; reprinted from *Zeitschrift fuer Flugtechnik und Motorluftschiffahrt,* Aug. 28, 1926, pp. 342–345.

[7]Van der Hegge Zijnen, B. G., "Determining the Velocity Distribution in the Boundary Layer of an Airfoil Fitted with a Rotary Cylinder," NACA TM 411, 1927; reprinted from *De Ingenieur*, Oct. 23, 1926.

[8]Ringleb, F. O., "Separation Control by Trapped Vortices," *Boundary Layer and Flow Control,* Vol. 1, edited by G. V. Lachmann, Pergamon, Oxford, England, UK, 1961, pp. 265–294.

[9]Hurley, D. G., "The Use of Boundary Layer Control to Establish Free Stream-Line Flows," *Boundary Layer and Flow Control,* Vol. 1, edited by G. V. Lachmann, Pergamon, Oxford, England, UK, 1961, pp. 265–294.

[10]Krall, K. M., and Haight, C. H., "Wind Tunnel Tests of a Trapped Vortex-High Lift Airfoil," Advanced Technology Center, Inc., ATC Rept. B-94300/3TR-10, Laguna Hills, CA, 1972.

[11]Gleason, M., and Roskam, J., "Preliminary Results of Some Experiments with a Vortex Augmented Wing," National Business Aircraft Meeting, SAE Paper 720321, Wichita, KS, March 1972.

[12]Cox, J., "The Revolutionary Kasper Wing," *Sport Aviation,* Vol. 11, July 1973, pp. 10–16.

[13]Kasper, W. A., "Some Ideas of Vortex Lift," National Business Aircraft Meeting, SAE Paper 750547, Wichita, KS, April 8–11, 1975.

[14]Chang, P. K., *Control of Flow Separation,* McGraw-Hill, New York, 1976, pp. 291–297, 412–444.

[15]Kruppa, E. W., "A Wind Tunnel Investigation of the Kasper Vortex Concept," AIAA 13th Annual Meeting and Display, AIAA Paper 77-310, Washington, DC, Jan. 1977.

[16]Saffman, P. G., and Sheffield, J. S., "Flow over a Wing with an Attached Free Vortex," *Studies in Applied Mathematics,* Vol. 57, No. 2, 1977, pp. 107–117.

[17]Rossow, V. J., "Lift Enhancement by an Externally Trapped Vortex," *Journal of Aircraft,* Vol. 15, No. 9, 1978, pp. 618–625.

[18]Mattick, A. A., and Stollery, J. L., "Increasing the Lift: Drag Ratio of a Flat Delta Wing," *Aeronautical Journal,* Oct. 1981, pp. 379–386.

[19]Saffman, P. G., and Tanveer, S., "Prandtl-Batchelor Flow Past a Flat Plate with a Forward-Facing Flap," *Journal of Fluid Mechanics,* Vol. 143, June 1984, pp. 351–365.

[20]Saffman, P. G., and Tanveer, S., "Vortex Induced Lift on Two Dimensional Low Speed Wings," *Studies in Applied Mathematics,* Vol. LXXI, No. 1, 1984, pp. 65–78.

[21]Rao, D. M., and Johnson, T. D., Jr., "Investigation of Delta Wing Leading-Edge Devices," *Journal of Aircraft,* Vol. 18, No. 3, 1981, pp. 161–167.

[22]Lamar, J. E., Schemensky, R. T., and Reddy, C. S., "Development of a Vortex-Lift Design Procedure and Application To A Slender Maneuver-Wing Configuration," *Journal of Aircraft*, Vol. 18, No. 4, 1981, pp. 259–266.

[23]Marchman, J. F., III, "Effectiveness of Leading-Edge Vortex Flaps on 60 and 75 Degree Delta Wings," *Journal of Aircraft,* Vol. 18, No. 4, 1981, pp. 280–286.

[24]Reddy, C. S., "Effect of Leading-Edge Vortex Flaps on Aerodynamic Performance of Delta Wings," *Journal of Aircraft,* Vol. 18, No. 9, 1981, pp. 796–798.

[25]Streeter, V. L., *Fluid Dynamics*, McGraw-Hill, New York, 1948, pp. 85–181.

[26]Lamb, H., *Hydrodynamics*, Dover, New York, 1932, pp. 224–229.

[27]Rossow, V. J., "Conformal Mapping for Potential Flow about Airfoils with Attached Flap," *Journal of Aircraft,* Vol. 10, No. 1, 1973, pp. 60–62.

[28]Theodorsen, T., "Theory of Wing Sections of Arbitrary Shape," NACA TR 411, 1932.

[29]"Aerodynamic Characteristics of Airfoils-IV," NACA TR 244, 1926.